The Trade-off between Color Reproduction Accuracy and Image Sensor Noise

Hideyasu Kuniba [1] ***and Roy S. Berns*** [2]
[1] ***Nikon Corporation, Tokyo, Japan;***
[2] ***Munsell Color Science Laboratory, Center for Imaging Science, Rochester Institute of Technology, Rochester, New York, USA***

Abstract

Image quality captured with five different spectral sensitivities were examined. Images were created with an image sensor model using four spectral images and three exposure index values. A psychophysical experiment was conducted and interval scales of preference were derived. It was shown that, as the exposure index increased, the preferred image sensor parameters shifted to better noise but less accurate color reproduction though strong image dependence was also shown. The interval scales were modeled using color difference, noise amplitude and their covariance. According to the fitting result, it was shown that even though both color difference and noise were measured in the same units, the effect of noise on the image quality was about 40% or less unless the high level perception of human visual system came into play.

Introduction

Digital still cameras have been used widely for the last ten years and their technology has developed dramatically. The resolution of consumer digital still cameras has increased about ten times. Even a digital camera with a 12 M pixel image sensor is not uncommon on the market today. This enables users to print pictures from these cameras in large format. As a consequence, the user demand for high quality image capture is increasing. However, color reproduction and noise as well as resolution account for the image quality and increasing resolution results in a decrease in pixel size for a fixed sensor size. The design of spectral sensitivities impacts the color reproduction. On the other hand, a smaller pixel captures a smaller amount of photon energy increasing the likelihood of noisy images [1]. Photon counting at the sensor inherently contains uncertainty, known as photon shot noise. As a result, even a perfect sensor will exhibit noise fluctuation due to photon shot noise. When considering a color image sensor, the captured signal should be transformed in order to represent proper color reproduction. This transformation depends on the sensor's spectral sensitivities and modulates noise components [2]. Accordingly, the design of spectral sensitivity should consider both colorimetric and noise performance and it was shown that though the R peak wavelength of 600nm was the best in terms of the color reproduction accuracy, a RGB color image sensor with a longer R peak wavelength suppressed noise along the a^* axis [3]. But the optimized color image sensor sensitivities with regard to the overall image quality including their color reproduction and noise is not obvious and requires psychophysical experiments.

In this research, a psychophysical preference experiment was conducted to investigate the trade-offs between color accuracy and image noise considering photon shot noise. A paired comparison experiment was conducted with simulated natural scenes of different RGB spectral sensitivity parameters and capturing conditions. The resulted quality scales were modeled with the color difference from the colorimetric image and the noise amplitude of the sensor model.

Model and Method

Image Sensor Model

A Gaussian function was used to define the spectral sensitivity curves of RGB sensors, expressed as,

$$S_i(\lambda) = \exp\left(-\frac{(\lambda-\lambda_i)^2}{w_i^2}\right), \tag{1}$$

where λ, λ_i, w_i are wavelength, peak wavelength and width, respectively, and $i = R, G, B$. These were combined with an IR cut-off filter (Fig. 1). The color transformation from camera RGB to

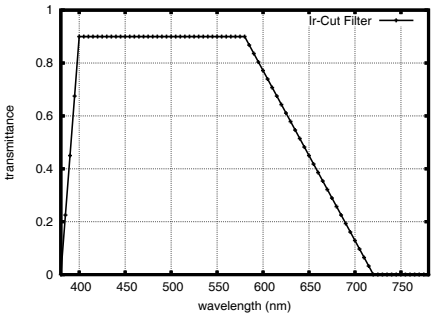

Figure 1. *IR cut filter model*

XYZ was defined as,

$$\begin{pmatrix} X/X_n \\ Y/Y_n \\ Z/Z_n \end{pmatrix} = \begin{pmatrix} m_1 & m_2 & m_3 \\ m_4 & m_5 & m_6 \\ m_7 & m_8 & m_9 \end{pmatrix} \begin{pmatrix} R/R_n \\ G/G_n \\ B/B_n \end{pmatrix}, \tag{2}$$

and

$$m_1 + m_2 + m_3 = m_4 + m_5 + m_6 = m_7 + m_8 + m_9 = 1,$$

where the suffix n means the value of white. This matrix definition ensures that the camera white is always mapped to the standard colorimetric white. The matrix was optimized to minimize the average CIE94 [7] color differences of the GretagMacbeth ColorChecker Color Rendition Chart for the 1931 CIE standard colorimetric observer and CIE Illuminant D65.

The signal from an image sensor contains two types of noise components: signal independent and signal dependent. The former includes dark current noise, reset noise and amplifier noise.

The latter includes photon shot noise. The variance of photon shot noise is proportional to the signal because the observed photon count follows Poisson statistics. Its variance is n when n photons should be observed on average. Given a spectral irradiance $I(\lambda)$[W/m^2/m], a spectral reflectance ratio $R(\lambda)$ of an object, spectral quantum efficiency $Q_i(\lambda)$ of an image sensor and an exposure time t[s], the photon count n_i at a pixel whose pixel area is l^2 (pixel pitch is l[m]) is expressed as

$$n_i = \int \frac{I(\lambda)R(\lambda)\, t\, l^2}{hc/\lambda} \cdot Q_i(\lambda)\, d\lambda, \tag{3}$$

where c is the speed of light, h is Planck's constant and $i = R,G,B$. The quantum efficiencies of each channel $Q_i(\lambda)$ were estimated by dividing the spectral sensitivities by λ and normalizing the maximum efficiency to 0.27 [8]. The numerator of the Eq. (3) is the photon energy falling onto one pixel. It is divided by the energy of a photon to give the incoming photon count on the pixel. Then incoming photon count is multiplied by the quantum efficiency to give the average count of the observed photons. In order to calculate photon count, the spectral irradiance was calculated from relative spectral power distributions and the definition of the focal plane exposure $H = 10/I_{\mathrm{EI}}$ [lm $\cdot$ m^{-2} $\cdot$ s] [9]. Thus, Eq. (3) is expressed as

$$n_i = \frac{l^2}{I_{\mathrm{EI}}} \frac{55.6}{683 \int I_0(\lambda)V(\lambda)d\lambda} \int \frac{I_0(\lambda)R(\lambda)}{hc/\lambda} \cdot Q_i(\lambda)\, d\lambda, \tag{4}$$

where I_{EI}, $I_0(\lambda)$, and $V(\lambda)$ are the exposure index, the relative illuminant spectral power distribution, and the spectral luminous efficiency function [10], respectively. When evaluating noise, the probability distribution of the signal was treated as a Gaussian random variable because Poisson statistics are well approximated by Gaussian statistics unless the count is very small. Thus the standard deviation σ_i due to noise around the average n_i is

$$\sigma_i = \sqrt{n_i + n_d}, \tag{5}$$

where n_i and n_d are the photon count and noise count that is independent of signal and has the same value for all channels, respectively, and the events of the former and the latter are independent. So the probability density of the observed signal is

$$P_i(x) = \frac{1}{\sqrt{2\pi(n_i+n_d)}} \exp\left(-\frac{(x-n_i)^2}{2(n_i+n_d)}\right). \tag{6}$$

Five sets of RGB spectral sensitivity parameters were used as shown in Table 1 and their quantum efficiency curves are shown in Fig. 2. These parameters were selected considering color reproduction error and noise using a metric m,

$$m = \sqrt{\Delta\bar{E}_{94}^2 + \alpha\ \bar{\sigma}_{94}^2}, \tag{7}$$

where $\Delta\bar{E}_{94}$ and $\bar{\sigma}_{94}$ are the average color difference and noise standard deviation in CIE94 units, respectively, for the Macbeth ColorChecker with a pixel pitch 4μm sensor at ISO1600 [3]. For a set of RGB spectral sensitivity parameters, $\Delta\bar{E}_{94}$ was derived as a residual color difference after the optimization of the color transformation matrix. On the other hand, capturing conditions such as pixel pitch, dark noise level, and exposure index were also required to calculate $\bar{\sigma}_{94}$. Different capturing conditions will give different $\bar{\sigma}_{94}$ values. Thus $\Delta\bar{E}_{94}$ and $\bar{\sigma}_{94}$ were treated separately in Eq. (7) and combined with a weighting factor α. When $\alpha = 0$, noise was not considered and as α increased, the image sensor showed less noise but worse color reproduction accuracy. The five parameter sets in Table 1 were selected according to the metric m for each α value from 16,500 sets whose parameter ranges were $\lambda_R = 590$–690, $\lambda_G = 540$–560, $\lambda_R = 430$–460, $w_{R,G,B} = 30$–70 each 10nm step. When the $\alpha = 0$, the peak wavelengths of RGB channels were 600nm, 550nm, 450nm, respectively. Quan, et al. [4] reported quite similar optimized result using μ-factor [5] and UMG [6]. In general, the peak wavelengths for the blue and green channels were nearly independent of noise, and thus, were almost fixed for this research.

Table 1. Spectral Sensitivity Parameters

α type	λ_R	λ_G	λ_B	w_R	w_G	w_B
0.0	600	550	450	60	50	30
0.125	620	540	450	50	40	30
0.25	630	540	450	50	40	30
0.5	640	540	450	50	40	30
1.0	650	550	450	50	40	40

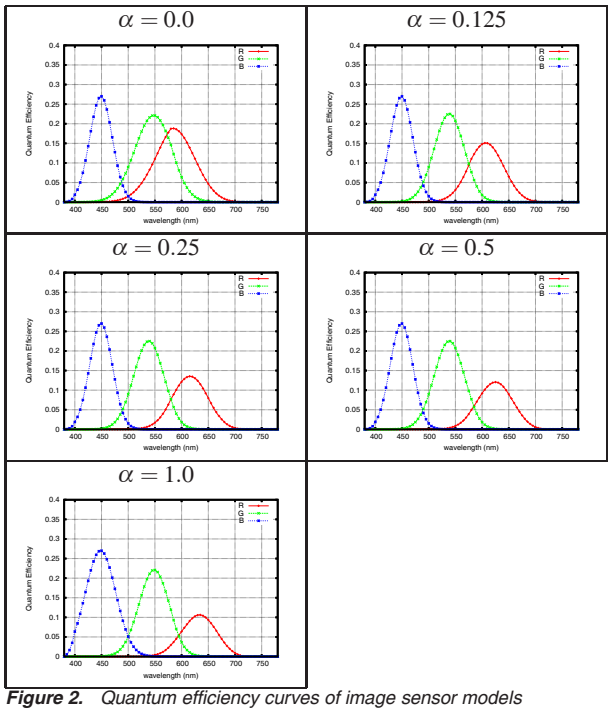

Figure 2. *Quantum efficiency curves of image sensor models*

Test Images

Spectral images from Chiba University Miyake Laboratory's standard spectral image data were used [11] [12]. Each is composed of five image bands, correction data of the sensor's nonlinearity, an estimation matrix, and the spectral power distribution of the illuminant. The spectral reflectance was recovered by,

$$\hat{\mathbf{R}} = \mathbf{I}^{-1}\mathbf{W}\mathbf{g}', \tag{8}$$

where $\mathbf{g}'$, $\mathbf{W}$, $\mathbf{I}$, $\hat{\mathbf{R}}$ are the linearized image data, the estimation matrix, the diagonal matrix of the illuminant, and the reconstructed spectral reflectance, respectively. Four images were selected from the eight standard images, "Oil Paint," "Fruits," "Portrait," and "Wool" (Fig. 3). "Fruit" and "Wool" have high reflectance ratio near the infrared region and this affected the color reproduction of image sensors whose red peak wavelengths were longer than 600nm. Of three available dimensions 764×508, 1528×1016, and 3056×2032, the images of 1528×1016 were used. The spectral image data $\hat{R}(x,y,\lambda)$ were substituted for $R(\lambda)$ of Eq. (4) to simulate the image sensor output. Test images were created from the four spectral images with the five spectral sensitivity parameters (Table 1) for a 4 μm pitch image sensor at ISO1600, 3200 and 6400.

Figure 3. *The four images used from Miyake Lab's spectral image data*

Experimental Procedures

A forced choice, paired comparison experiment was conducted to investigate the preferred image sensor parameters for these images at each ISO sensitivity setting. Observers were instructed to select the preferred image considering both color reproduction and noise. During this experiment, no reference was presented; thus the observers' selection was based on image preference for typical consumer imagery. Each session contained 40 pairs. These images were displayed on an IBM T221 22.1-inch QXGA-W (3840×2400 pixels) LCD whose pixel density was 204 dpi (Fig. 4). The viewing distance was about 1–1.5 ft. The pixel density and the viewing distance were important for this experiment because noise exhibited high frequency texture on an image and its appearance depended on the pixel density and the viewing distance. When printing a 10M pixel image using a consumer photo printer on a 13"$\times$19" paper, 204 dpi is a suitable resolution. The LCD was calibrated and fitted with an LCD model [13], then the tristimulus values of the images were converted to digital counts using the inverse model. The average CIEDE2000 over the Macbeth ColorChecker was 1.4.

Figure 4. *A screen-shot of the experiment*

Results and Discussions

Twelve observers took part in the experiment. Using Thurstone's law of comparative judgment (Case V) [14], interval scales were derived as shown in Fig. 5, where the green solid lines connect the calculated scales for different sensors and the red error bars show the 95% confidence interval; the blue dashed lines show a model, described below. Most observers commented that they did not see noise so much. This was due the high resolution (204 dpi) of the LCD. But it can be seen that even though the scales show an obvious image dependence, there is a general trend that as the ISO sensitivity value became larger, sensors of $\alpha = 0$ were assigned relatively lower scale values, This is reasonable because in case of $\alpha = 0$, noise was not considered when optimizing the spectral sensitivity of the sensor. As α became larger, noise was considered more and the color reproduction suffered. At ISO1600, which was the least noisy capturing condition, there were no significant differences of the preference scale values for "Oil Paint" and "Portrait" between image sensor models. At ISO6400, which was the most noisy capturing condition, for "Oil Paint," the image sensor model of $\alpha = 0.125$ was assigned marginally better scale values than that of $\alpha = 0$ but sensors of $\alpha = 0.25,\ 0.5,\ 1.0$ did not have statistically significant differences from $\alpha = 0$. For "Portrait," sensors of $\alpha = 0.25,\ 0.5,\ 1.0$ had better scale values than $\alpha = 0$. On the other hand, for "Fruit" at ISO1600, the image sensor models of $\alpha = 0,\ 0.125$ were assigned better scale values than that of $\alpha = 1.0$. Because "Fruit" contained objects with high near IR reflectance, the sensor model of $\alpha = 1.0$ whose red peak wavelength was 650nm suffered large color difference. For "Wool" at ISO1600, the similar scale values were derived. Though "Wool" also contained objects with high near IR reflectance, this result is interesting because no reference image was presented in this experiment and "Wool" did not contain memory colors. Thus the scale of "Wool" was a function of a preference for blue or for purple. At ISO6400 for "Fruit," the sensor of $\alpha = 0.125$ was assigned marginally better scale value than $\alpha = 0,\ 1.0$ but the differences between sensors of $\alpha = 0.25,\ 0.5,\ 1.0$ and $\alpha = 0$ were not significant. For "Wool," the differences between models were statistically insignificant. At ISO3200, the interval scales were almost halfway between ISO1600 and ISO6400 for all the four images.

Several image quality models were already proposed, such as S-CIELAB [15] and iCAM [16]. They were modeled with regard to the human visual system. But, in this research, the image quality was modeled with regard to the image sensor to see how the spectral sensitivity affected the image quality. In order to describe these results, color difference and noise amplitude were assumed the only contributors to the total image quality. The color difference $\Delta\bar{E}_{94,\mathrm{im}}$ was defined as the averaged pixel-wise CIE94 color difference from the colorimetric reproduction. It depended on each image and the sensor as shown in Table 2. The noise amplitude $\bar{\sigma}_{94}$ was defined as an average standard deviation due to noise for the Macbeth ColorChecker in the CIE94 units, and depended on each sensor and ISO sensitivity as shown in Table 3. The simplest formula of the interval scale was adding these two as $(-\Delta\bar{E}_{94,\mathrm{im}} - \beta\bar{\sigma}_{94})$, where β was multiplied to $\bar{\sigma}_{94}$ because noise should not be as perceptible as color difference due to its high frequency components. Negative values were used because the larger the $\Delta\bar{E}_{94,\mathrm{im}}$ and the $\bar{\sigma}_{94}$, the smaller the image quality. However, this did not fit the results. Thus, their covariance, defined by the geometric mean term of $\Delta\bar{E}_{94,\mathrm{im}}$ and $\bar{\sigma}_{94}$, was also considered. Then an interval scale model s was written as,

$$s = -\Delta\bar{E}_{94,\mathrm{im}} - \beta\ \bar{\sigma}_{94} - \varepsilon\ \sqrt{\Delta\bar{E}_{94,\mathrm{im}} \cdot \bar{\sigma}_{94}} + C \qquad (9)$$

where β, ε, C are two model parameters and an offset constant, respectively. The constant C was added to make the minimum score zero. The color differences averaged over an image were assumed to be the nominal interval scale and the effect of noise amplitudes would be discounted according to the viewing condition because noise exhibited high frequency components and its perception suffered spatial averaging. The geometric mean term should account for the non-linear correlation between color difference and noise to image quality. The factors β and ε were image dependent and could be explained through the understanding of the human visual system and the perception of image and noise. This will be a future work which will need intensive psychophysical experiments.

The β, ε were estimated to minimize the least square error for each image and are shown in Table 4 and s values are shown in Fig. 5. Even though it was a simple model, Eq. (9) well described the experimental results. The discounting factor β ranged from 0.32 to 0.39 for "Oil Paint," "Fruit" and "Portrait" but almost zero for "Wool" while the factor of color difference was assumed to be unity. Thus the noise itself did not have any effect on the image quality for "Wool." The correlation factors ε were negative and their amplitudes were 0.14 and 0.13 for "Oil Paint" and "Fruit," respectively, which were less than half of their β values. In case of "Portrait," the amplitude of correlation factor was 0.76 and much larger than the β (0.34). This could be caused by the high level perception in the human visual system when viewing portraiture. In case of "Wool," the amplitude of correlation factor was 0.67. In this case β was almost zero. Even though "Wool" showed significant difference in color for different αs, observers had difficulty in judging the preferred image of "Wool" because, without reference or memory colors, they did not know the original colors. This might have confused their judgment.

Conclusions

A psychophysical experiment was conducted to examine the effect of image sensor noise and the color reproduction on image quality as a function of the sensor sensitivities. Specifically, optimum spectral sensitivities for different exposure indices (ISO sensitivities) were examined. It was shown that, as the exposure index increased, the optimum image sensor parameters shifted to better noise but less accurate color reproduction ones though strong image dependence was also shown. Interval scales of the preference were modeled with a function of the color difference from the colorimetric reproduction and the noise fluctuation of the sensor model. Then it was indicated that the noise fluctuation corresponded to about 30–40% of the color difference though this should have been dependent on viewing conditions and on image content.

Table 2. Averaged pixel-wise color difference $\Delta\bar{E}_{94,\mathrm{im}}$

Image	α				
	0.0	0.125	0.25	0.5	1.0
Oil Paint	0.17	0.36	0.55	0.76	1.23
Fruit	0.35	0.70	1.22	1.78	2.63
Portrait	0.25	0.60	1.00	1.32	1.99
Wool	0.39	0.94	1.89	2.83	4.16

Table 3. Noise amplitude $\bar{\sigma}_{94}$ for each capturing condition

ISO	α				
	0.0	0.125	0.25	0.5	1.0
1600	8.14	6.38	6.16	6.02	5.79
3200	11.36	8.91	8.62	8.44	8.12
6400	15.82	12.40	12.04	11.85	11.35

Table 4. Estimated Model Parameters

	Oil Paint	Fruit	Portrait	Wool
β	0.39	0.32	0.34	−0.02
ε	−0.14	−0.13	−0.76	−0.67

Acknowledgements

The authors would like to thank Prof. Mark D. Fairchild for his advice, Mr. Lawrence Taplin for the setup of the experiment, Mr. Abhijit Sakar for allowing us to use his paired comparison software, and those who participated as observers in Munsell Color Science Laboratory, Rochester Institute of Technology.

References

[1] F. Xiao, J. E. Farrel and B. A. Wandell, "Psychophysical thresholds and digital sensitivity: the thousand photon limit," *Proceedings of SPIE-IS&T Electronic Imaging* SPIE **5678**, pp. 75–84, 2005.

[2] P. D. Burns and R. S. Berns, "Error Propagation Analysis in Color Measurement and Imaging," *Color Research and Application*, **22(4)**, pp. 280–289, 1997.

[3] H. Kuniba and R. S. Berns, "Spectral Sensitivity optimization of color image sensor considering photon shot noise," *Proceedings of SPIE*, **6817**, 68170P, 2008.

[4] S. Quan, N. Ohta and N. Katoh, "Optimization of Camera Spectral Sensitivities," *IS&T/SID Eighth Color Imaging Conference*, pp. 273–278, 2000.

[5] P. L. Vora and H. J. Trussell, "Measure of Goodness of a Set of Color-Scanning Filters," *J. Opt. Soc. Am. A*, **10**, pp. 1499–1508, 1993.
[6] S. Quan, "Evaluation and Optimal Design of Spectral Sensitivities for Digital Color Imaging," Ph.D dissertation, Munsell Color Science Laboratory, Rochester Institute of Technology, 2002.
[7] R. S. Berns, *Billmeyer and Saltzman's Principles of Color Technology 3rd ed.*, Section 4.D, John Willy & Sons, New York, 2000.
[8] K. Parulski and K. Spaulding, "Color image processing for digital cameras" in *Digital Color Imaging Handbook*, G. Sharma, ed., pp.727–757, CRC Press, Florida, 2002.
[9] *Photography – Digital still cameras – Determination of exposure index, ISO speed ratings, standard output sensitivity, and recommended exposure index*, ISO12232:2006(E), 2006-10-01.
[10] *International Lighting Vocabulary*, CIE Publ. No. 17.4, 1987.
[11] *Introduction to Multispectral Imaging* (in Japanese), Y. Miyake, ed., University of Tokyo Press, 2006.
[12] T. Fujimaki, K. Ishii, T. Ikeda, N. Tsumura and Y. Miyake, "Proposals of Standard Spectral Image and its Application to Designing of CCD Camera," *IS&T's 2003 PICS Conference Proceedings*, pp. 496–499, 2003.
[13] E. A. Day, L. Taplin and R. S. Berns, "Colorimetric Characterization of a Computer-Controlled Liquid Crystal Display," *Color Research and Application*, **29(5)**, pp. 365–373, 2004.
[14] G. A. Gescheider, *Psychophysics: The fundamentals, Third Ed.*, Section 9, Lawrence Erlbaum Associates, Inc., 1997.
[15] X. M. Zhang, B. A. Wandell, "A spatial extension to CIELAB for digital color imaging reproduction," *Proceedings of the SID Symposiums*, pp.731–734, 1996.
[16] M. D. Fairchild and G. M. Johnson, "Measuring images: Differencec, Quality, and Appearance," *Proceedings of SPIE-IS&T Electronic Imaging* SPIE **5007**, pp. 51–60, 2003.

Author Biography

Hideyasu Kuniba received his BS and MS degree in astronomy from Kyoto University, Kyoto, Japan. He develops image processing algorithms of DSCs in Nikon. He was a visiting researcher at Munsell Color Science Laboratory, Rochester Institute of Technology from 2007 to 2008.

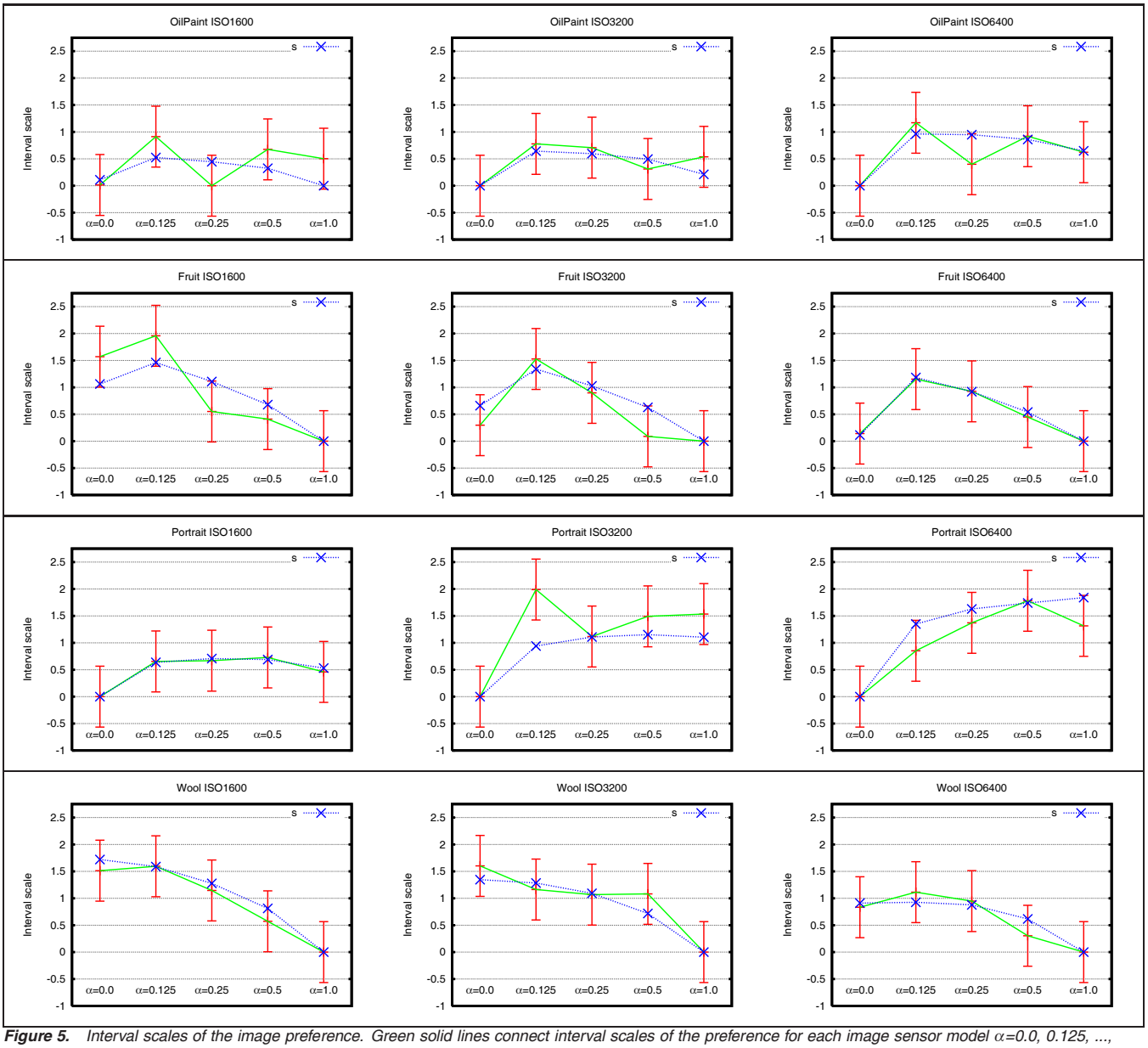

Figure 5. *Interval scales of the image preference. Green solid lines connect interval scales of the preference for each image sensor model α=0.0, 0.125, ..., 1.0, and red error bars are 95% confidence interval. Blue dashed lines connect estimated interval scale values using Eq. (9). Results are statistically significantly different when error bars do not overlap.*